

Synthesis, characterization and thermal properties of novel epoxy containing silicon and phosphorus nanocomposites by sol–gel method

Chin-Lung Chiang^{a,b}, Chen-Chi M. Ma^{a,*}

^a Department of Chemical Engineering, National Tsing-Hua University, Hsin-Chu 30043, Taiwan, ROC

^b Department of Industrial Safety and Health, Hung Kuang Institute of Technology, Sha-Lu 433, Taiwan, ROC

Received 4 December 2001; received in revised form 16 April 2002; accepted 18 April 2002

Abstract

Organic–inorganic hybrids were prepared using diglycidyl ether of bisphenol A (DGEBA) type epoxy and tetraethoxysilane via the sol–gel process. The DGEBA type epoxy was modified by a coupling agent to improve the compatibility of the organic and inorganic phases. The sol–gel technique was used successfully to incorporate silicon and phosphorus into the network of hybrids increasing flame retardance.

Fourier transform infrared spectroscopy and ²⁹Si nuclear magnetic resonance spectroscopy were used to characterize the structure of the hybrids. In condensed siloxane species for TEOS, silicon atoms through mono-, di-, tri-, and tetra-substituted siloxane bonds are designated as Q¹, Q², Q³, Q⁴, respectively. For 3-isocyanatopropyltriethoxysilane and diethylphosphatoethyltriethoxysilane, mono-, di-, tri-, tetra-substituted siloxane bonds are designated as T¹, T², T³. Results revealed that Q⁴, Q³, T³ are the major environments forming a network structure. The morphology of the ceramer was examined by scanning electron microscopy and Si mapping. Particle sizes were below 100 nm. The hybrids were nanocomposites. The char yield of pure epoxy resin was 14.8 wt.% and that of modified epoxy nanocomposite was 31 wt.% at 800 °C. A higher char yield enhances the flame retardance. Values of limiting oxygen index of pure epoxy and modified epoxy nanocomposites are 24 and 32, respectively, indicating that modified epoxy nanocomposites possess better flame retardance than the pure epoxy resin.

© 2002 Elsevier Science Ltd. All rights reserved.

Keywords: Epoxy; Hybrid ceramers; Flame retardance; Silicon; Phosphorus; Nanocomposite; Sol–gel technique

1. Introduction

Over the past decade, the synthesis and characterization of inorganic–organic hybrid materials by the sol–gel process have received considerable attention [1–7]. This interest relies upon the unique opportunity of combining the remarkable properties of inorganic glasses and organic polymers in a controlled way. For instance, flexi-

ble polymers with high modulus, together with the high thermal stability and good optical properties of inorganic glasses can be prepared. The main physical, mechanical, thermal and optical properties of these composites, known as ceramers, are heavily dependent on phase continuity, mean size, molecular mixing at the phase boundaries and intrinsic properties of the constitutive components.

Epoxy resins are globally used on a large scale for adhesive, laminating, coating, and casting applications. Several methods have been adopted to enhance the thermal properties of epoxy resins and thus meet some application requirements [8–10]. A further requirement

* Corresponding author. Tel.: +886-3-5713058; fax: +886-3-5715408.

E-mail address: ccma@che.nthu.edu.tw (C.-C.M. Ma).

that has recently gained importance is the need of flame resistance, and imparting flame retardance into epoxy resins has attracted much attention [11–14].

The sol–gel process is well known to proceed by hydrolysis and condensation reactions, which are governed by value of pH, solvent, water to alkoxide ratio, concentration of the reactants, catalyst, and temperature [15–18]. An organic component, involved during a sol–gel process, influences the reaction kinetics, morphology and the physical properties of resultant hybrid materials. The structure–property relationship of organic–inorganic sol–gel composites with either hydrogen bonding or weaker interaction between organic and inorganic components has received considerable attention [19,20]. This work demonstrates that covalent bonding between polymer and silica components occurs. The synthesis, characterization and properties of novel epoxy resins, containing silicon and phosphorus nanocomposites, are elucidated by the sol–gel method, and the presence of silicon and phosphorus enhances resistance to flames. The epoxy resin is modified to improve the interaction between organic and inorganic phases.

2. Experimental

2.1. Materials

The epoxy resin used in this study was the diglycidyl ether of bisphenol A (DGEBA, NPEL-128), which was generously provided by Nan Ya Plastics Corporation, Taiwan. The coupling agent, 3-isocyanatopropyltriethoxysilane, was purchased from United Chemical Technologies, Inc., USA. Diethylphosphatoethyltriethoxysilane was obtained from Gelest, Inc, USA. Tetraethoxysilan (TEOS) was purchased from (Acros Organics Co., USA).

2.2. Preparation of hybrid ceramer

The hybrid creamers were prepared by mixing two solutions, A and B. Solution A consisted of modified epoxy resin and THF. The modified epoxy resin was synthesized as follows: 0.4 g 3-isocyanatopropyltriethoxysilane (equivalent weight 247 g) was added to 10 g DGEBA type epoxy resin (equivalent weight 180 g) at 60°, and was then stirred for 4 h until the characteristic peak of the NCO group disappeared. Solution B, was composed of H₂O/diethylphosphatoethyltriethoxysilane/HCl/TEOS, in a molar ratio 9:1:0.63:1. HCl was used as the catalyst for hydrolysis. 3.4 g 4,4'-diaminodiphenylsulfone (equivalent weight 62 g) was poured into the mixture of solutions A and B. 4,4'-diaminodiphenylsulfone was used as the curing agent of the modified epoxy resin. 3-Isocyanatopropyltriethoxysilane/epoxy resin/4,4'-diaminodiphenylsulfone were used with an

equivalent ratio of 0.3:1:1. The mixture was stirred until the solution became clear. The solution was cast into aluminum dishes to gel at room temperature. The wet gel was aged at room temperature for 48 h, and was then dried at 80 °C for 24 h. The samples were placed in a vacuum oven at 150 °C for 24 h.

2.3. Reaction scheme

Epoxy resin containing silicon and phosphorus hybrid was prepared as described in Scheme 1.

2.4. Fourier transform infrared spectroscopy

Fourier transform infrared spectroscopy (FT-IR) spectra of the hybrid ceramers were recorded between 4000 and 400 cm⁻¹ on a Nicolet Avatar 320 FT-IR spectrometer. Thin films were prepared by the solution-casting method. A minimum of 32 scans was signal-averaged with a resolution of 2 cm⁻¹ at the 4000–400 cm⁻¹ range.

2.5. Solid state ²⁹Si nuclear magnetic resonance spectroscopy

²⁹Si nuclear magnetic resonance spectroscopy (²⁹Si NMR) was performed using a Bruker DSX-400WB. The samples were treated at 180 °C for 2 h and then ground into fine powder.

2.6. Morphological properties

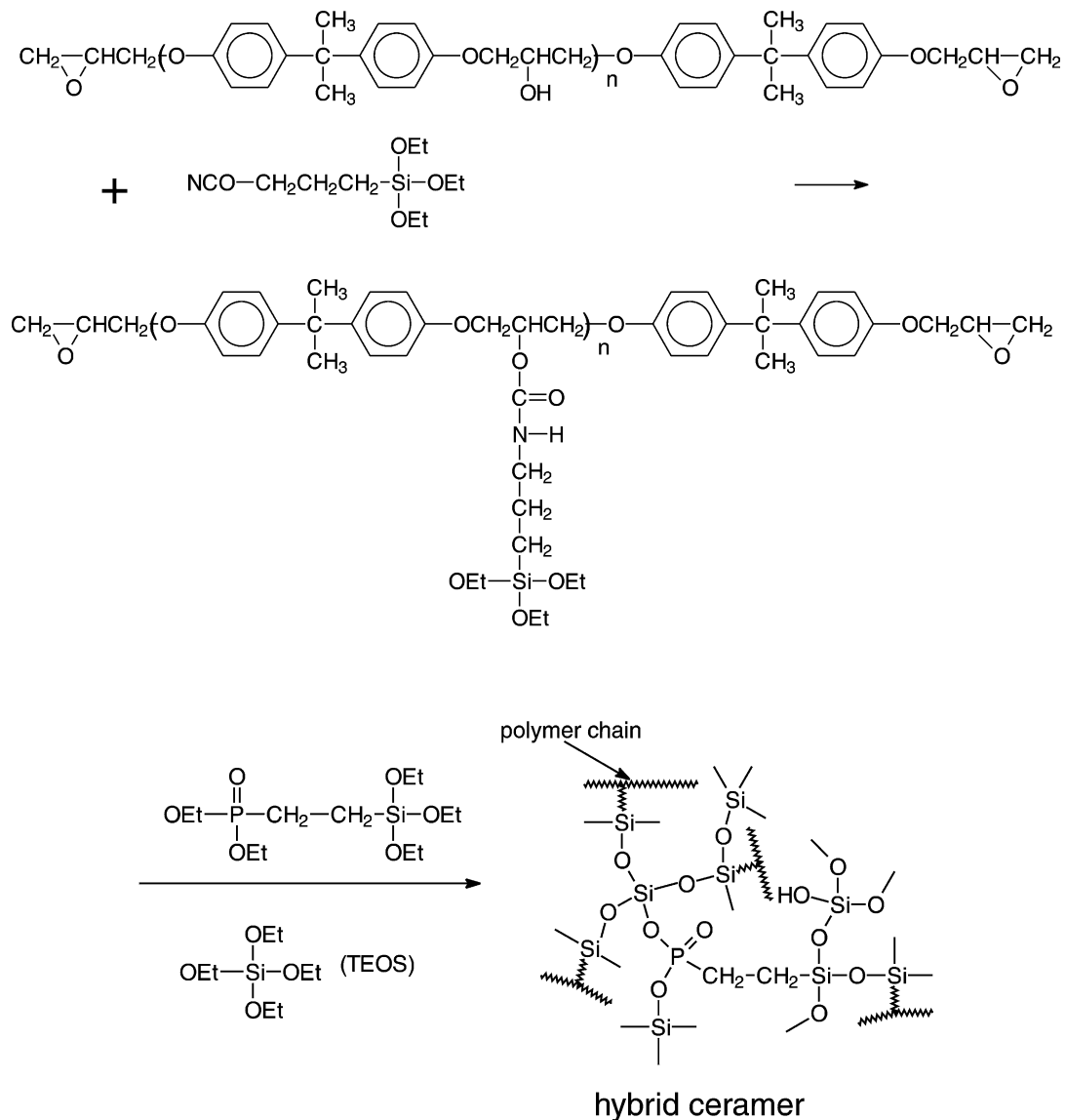
The morphology of the fracture surface of the composite was examined using a scanning electron microscope (SEM; JEOL JSM 840A, Japan).

2.7. Si mapping technology

The distributions of Si atoms in the hybrid creamers were obtained by SEM EDX mapping (JEOL JSM 840A, Japan). The white points in the figures denote Si atoms.

2.8. Thermogravimetric analysis

The nanocomposite was thermally degraded by thermogravimetric analysis (TGA) (DU-Pont-951) from room temperature to 800 °C, at a heating rate of 10 °C/min in a nitrogen atmosphere. The samples were treated at 180 °C for 2 h and then ground into fine powder. The measurements were taken using 6–10 mg samples. Weight-loss/temperature curves were recorded.



Scheme 1.

2.9. Limiting oxygen index test

The limiting oxygen index (LOI) is defined as the minimum fraction of O_2 in a mixture of O_2 and N_2 that will just support flaming combustion. The LOI test was performed according to the testing procedure of the ASTM D 2836 oxygen index method, with a test specimen bar 7–15 cm long, 6.5 ± 0.5 mm wide, and 3.0 ± 0.5 mm thick. The sample bars were suspended vertically and ignited by a bunsen burner. The flame was removed and the timer was started. The concentration of oxygen was increased if the flame on the specimen was extin-

guished before burning for 3 min or burning away 5 cm of the bar. The oxygen content was adjusted until the limiting concentration was determined.

3. Results and discussion

3.1. Characterization

Fig. 1 presents FT-IR spectra of the reaction between epoxy resin and 3-isocyanatopropyltriethoxysilane. The figure shows the disappearance of the characteristic

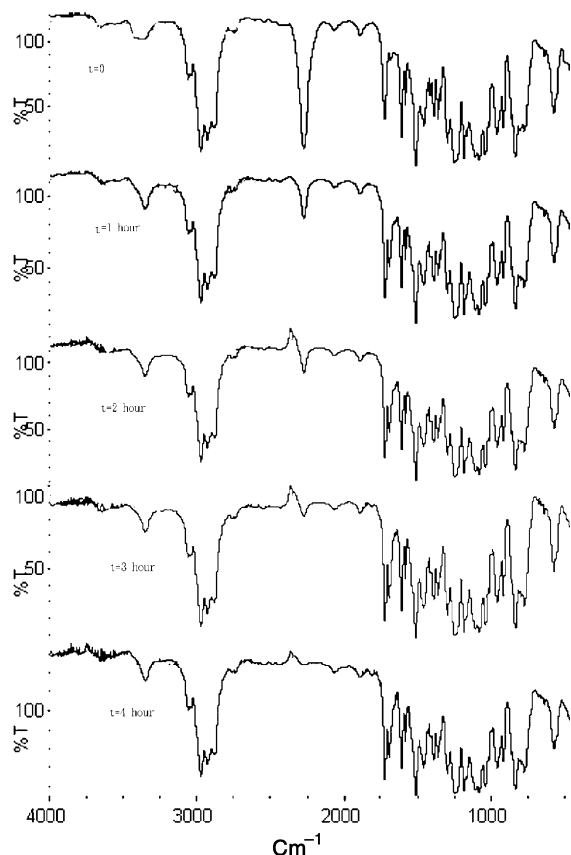


Fig. 1. FT-IR spectra of the reaction between epoxy resin and 3-isocyanatopropyltriethoxysilane.

peak of the NCO group of 3-isocyanatopropyltriethoxysilane at 2270 cm^{-1} . This phenomenon reveals that

epoxy resin has reacted with 3-isocyanatopropyltriethoxysilane.

Fig. 2 displays the solid-state ^{29}Si NMR spectrum of the epoxy nanocomposite. In condensed siloxane species for TEOS, silicon atoms through mono-, di-, tri-, and tetra-substituted siloxane bonds are designated as Q^1 , Q^2 , Q^3 , Q^4 , respectively. The chemical shifts of Q^2 , Q^3 , Q^4 are -91 , -101 , and -109 ppm respectively, and are in good agreement with the literature [19]. For 3-isocyanatopropyltriethoxysilane and diethylphosphatoethyltriethoxysilane, mono-, di-, tri-, tetra-substituted siloxane bonds are designated as T^1 , T^2 , T^3 . The chemical shifts of T^2 and T^3 are -56 and -65 ppm, respectively, and conform to the literature values [20]. Results revealed that Q^4 , Q^3 and T^3 are the major microstructures, forming the network structure.

3.2. Morphological properties

The compatibility of organic polymer and silica greatly affects thermal, mechanical and optical properties. The morphology of the fractured surfaces was observed by SEM, and using the mapping technique to elucidate the distribution of silica and the separation of microphase in the hybrid matrix. Fig. 3 presents an SEM photograph of the morphology of the composites. Fig. 4 shows Si mapping of epoxy nanocomposites. According to these figures, the particles were uniformly dispersed throughout the polymer matrix with sizes below 100 nm. This result revealed that the nanocomposites exhibit good miscibility between organic and inorganic phases. It is found that the particles are well distributed and are of different sizes. Two different components containing TEOS and diethylphosphatoethyltriethoxysilane participate in the sol-gel reaction. The sol-gel reaction con-

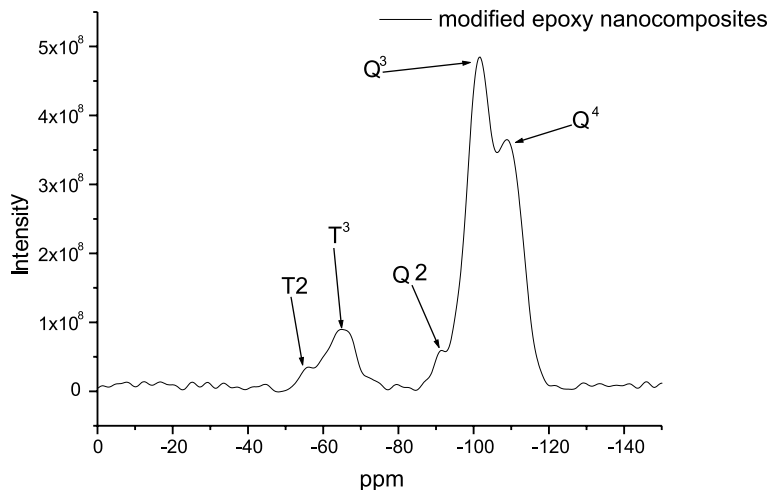


Fig. 2. Solid-state ^{29}Si NMR spectrum of modified epoxy nanocomposite.

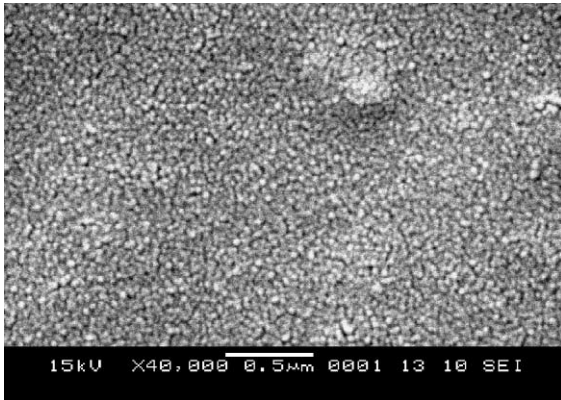
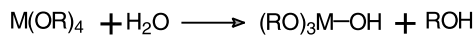


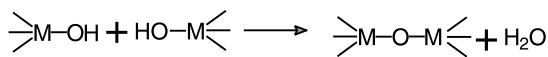
Fig. 3. SEM of modified epoxy nanocomposites.

sists of hydrolysis and condensation reactions. The hydrolysis and condensation reactions involved in the process may proceed as follows [21].

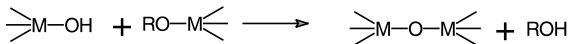
Hydrolysis



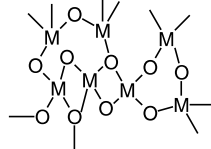
Condensation



and/or



Net Reaction



M=Si or Ti etc

Therefore, sol-gel reactions contain various degrees of hydrolysis and condensation. This leads to the production of particles of different sizes. The SEM micrograph was analyzed by Image-Pro Plus software (version 4.5, Media Cybernetic Co., USA). A particle size distribution is shown in Fig. 5. From this figure, the size of the majority of particles is 11–40 nm. Consequently, silica networks are restrained at the molecular level in modified epoxy nanocomposites. The nanocomposites were transparent.

3.3. Thermal stability and flame retardance

Fig. 6 shows TGA curves of pure epoxy resin and modified epoxy nanocomposites in a nitrogen

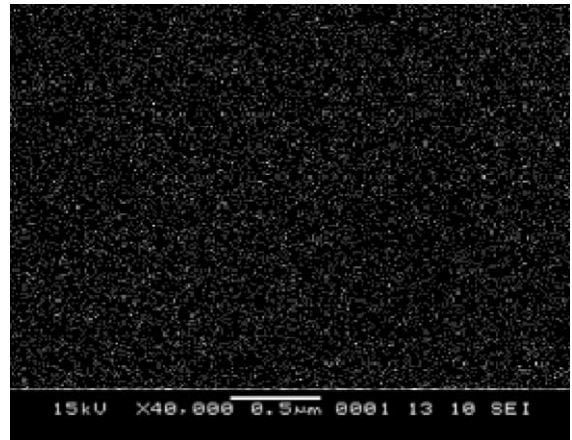


Fig. 4. Si mapping of modified epoxy nanocomposites.

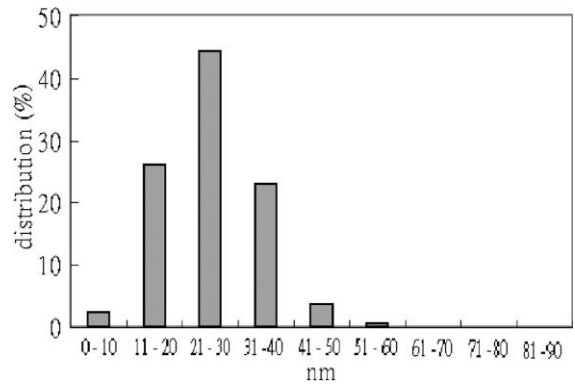


Fig. 5. Distribution of particle size.

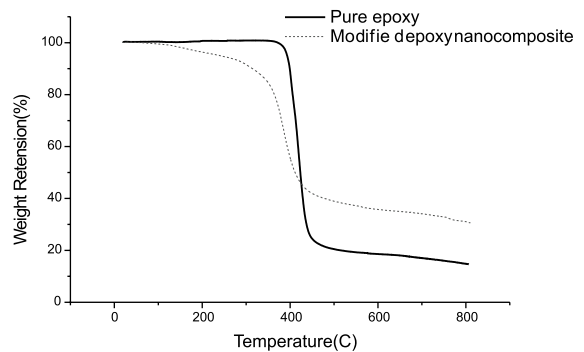


Fig. 6. TGA curve of pure epoxy resin and modified epoxy nanocomposite.

Table 1
Thermal properties of pure epoxy resin and modified epoxy nanocomposite

	Temperature of weight loss at 10% (°C)	Char yield (%)				LOI
		200 °C	400 °C	600 °C	800 °C	
Pure epoxy resin	399	100	88	19	14.8	24
Epoxy nanocomposite	313	96	56	36	31	32

atmosphere. The weight-loss curves for pure epoxy resin and modified epoxy nanocomposites imply a one-step degradation mechanism. Table 1 depicts the thermal properties of pure epoxy resin and modified epoxy nanocomposites. The values of $T_{d_{10}}$ (the temperature of degradation at which the weight loss is 10%) for pure epoxy and modified epoxy nanocomposites are 399 and 313 °C, respectively. The thermal stability of modified epoxy hybrid at a low temperature is not superior to that of the pure epoxy resin; however, the char yield of modified epoxy hybrid is higher than that of the pure epoxy resin at 800 °C. The behavior follows from the presence of P–C and P–O structures in the hybrid creamers. These structures act as weak links and are highly susceptible to chain scission during thermal degradation [22,23]. The char yield of pure epoxy is 14.8 wt.% and that of modified epoxy nanocomposite is 31 wt.% at 800 °C. Consequently, the thermal stability of epoxy nanocomposites at high temperatures exceeds that of pure epoxy. Flame resistance can be quantified from the char residue on pyrolysis. Van Krevelen established a linear relationship between LOI and char residue for halogen-free polymers [24]. Increasing the char formation can limit the production of combustible carbon-containing gases, decreasing the exothermicity due to pyrolysis reactions, and decreasing the thermal conductivity of the surface of burning materials [25]. A higher char yield will enhance flame retardance. The LOI of pure epoxy resin and modified epoxy nanocomposites are 24 and 32, respectively, indicating that modified epoxy nanocomposites exhibit better flame retardance than pure epoxy resin.

4. Conclusions

A novel epoxy resin containing silicon and phosphorus nanocomposites was prepared successfully by the sol–gel method. The hybrid creamer has a network structure and inorganic phases have a size of less than 100 nm. The hybrids were nanocomposites. The sol–gel technique was used to incorporate silicon and phosphorus into the network of hybrids, increasing the flame retardance. The thermal stability of epoxy nanocomposites at high temperature is higher than that of the pure epoxy resin.

References

- [1] Wikes GL, Huang HH, Glaser RH. In: Silicon-based polymer science, Advances in chemistry series 224. Washington, DC: American Chemical Society; 1990. p. 207–26.
- [2] Philip G, Schmidt H. *J Non-Cryst Solids* 1984;63:283.
- [3] Mark JE, Jiang C, Tang MY. *Makromol Chem* 1984;17:2616.
- [4] Brennan AB, Wikes GL. *Polymer* 1991;32:733.
- [5] Chujo Y, Ihara E, Kuse S, Suzuki K, Saegusa T. *Macromol Chem, Macromol Symp* 1991;42/43:303.
- [6] Girard-Reydet E, Lam TM, Pascault JP. *Macromol Chem Phys* 1994;195:149.
- [7] Ellsworth MW, Novak BM. *Polym Prepr* 1993;34:356.
- [8] Cadiz ASV, Martinez PA, Mantecon A. *Angew Makromol Chem* 1986;140:113.
- [9] Martinez PA, Cadiz V, Mantecon A, Serra A. *Angew Makromol Chem* 1985;133:97.
- [10] Mantecon A, Cadiz V, Serra A, Martinez PA. *Eur Polym J* 1987;23:481.
- [11] Mikroyannidis JA, Kourtidis DA. *J Appl Polym Sci* 1984;29:197.
- [12] Lewin M, Atlas SM, Pearce EH. In: Flame retardant polymeric materials. New York: Plenum; 1975. p. 22.
- [13] Mikroyannidis JA, Kourtidis DA. *Adv Chem Ser* 1984;208:351.
- [14] Chin WK, Hsau MD, Tsai WC. *J Polym Sci Chem Ed* 1995;33:373.
- [15] Brinker CJ, Scherer GW. *Sol–gel science, the physics and chemistry of sol–gel processing*. San Diego: Academic Press; 1990.
- [16] Schmidt H, Siefertling B, Philip G, Deichman K. In: Mackenzie DR, editor. *Ultrastructure processing of advanced ceramics*. New York: Wiley; 1988. p. 651.
- [17] Novak BM. *Adv Mater* 1993;5:422.
- [18] Mark JE, Lee CYC, Bianconi PA. *Hybrid organic–inorganic composites*, ACS Symp. Ser. 585. Washington, DC: American Chemical Society; 1995.
- [19] Brinker CJ, Scherer GW. *Sol–gel science, the physics and chemistry of sol–gel processing*. San Diego: Academic Press; 1990.
- [20] Joseph R, Zhang S, Ford W. *Macromolecules* 1996;29:1305.
- [21] Sarwar MI, Ahmad Z. *Eur Polym J* 2000;36:89.
- [22] Liu YL, Hsiue GH, Lan CW, Chiu YS. *Polym Degrad Stab* 1997;56:291.
- [23] Chang TC, Chiu YS, Chen HB, Ho SY. *Polym Degrad Stab* 1995;47:375.
- [24] Van Krevelen DW. *Polymer* 1975;16:615.
- [25] Pearce EM, Liepins R. *Environ Health Perspect* 1975;11:69.